

Device Guidelines for WDM Interconnects Using Silicon Microring Resonators

Nicolás Sherwood-Droz,^{1,*} Kyle Preston,^{1,*} Jacob S. Levy,¹ and Michal Lipson^{1,2}

¹School of Electrical and Computer Engineering, ²Kavli Institute at Cornell for Nanoscale Science, Cornell University, Ithaca, NY 14853

*These authors contributed equally to this work

Abstract: We derive guidelines for the WDM bandwidth, channel spacing, and optical power handling achievable in silicon nanophotonic devices for large-scale optical links or networks.

Introduction

Optical interconnects which utilize silicon nanophotonic devices have been proposed as a solution to provide high-bandwidth, low-power, and low-latency data communication for telecom, datacom, chip-to-chip, and on-chip applications. Many groups have proposed highly complex silicon photonic interconnection network designs [1-2], from which the microring resonator [3] has emerged as the key building block to enable efficient and scalable optical systems. The small size of the device enables low-power and space-efficient devices, and its wavelength selectivity allows for cascaded wavelength division multiplexing (WDM).

Design of such complex optical systems requires careful accounting of insertion losses, crosstalk, and nonlinear effects which has been lacking in many system-level publications to date. Here we describe the fundamental limits for number of WDM channels and power per channel when using building blocks that include silicon waveguides, silicon microring modulators and filters (Fig. 1(b)).

WDM Bandwidth

The bandwidth available for WDM is determined by the maximum free spectral range (FSR) of the microring, which is found for the smallest device size. We study the FSR by simulating the effective index and solving for the resonant wavelengths given by the resonator equation $m\lambda = 2\pi r n_{eff}$ where m is an integer, r is the radius of the ring, and $n_{eff}(\lambda, r, \dots)$ is the effective index which is a function of the waveguide cross-sectional geometry, as well as wavelength, radius, temperature, electron concentration, etc. The resonant wavelengths λ_m can be determined precisely if the full form of $n_{eff}(\lambda, r)$ is known within some range of radii and wavelengths.

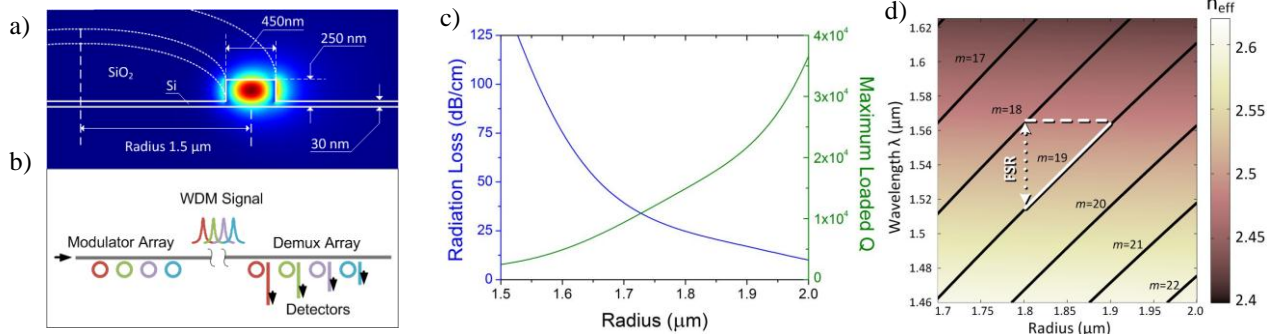


Fig. 1. (a) Schematic of a 450 nm × 250 nm silicon ring with 30 nm slab and surrounded by silicon dioxide, showing TE optical mode at $\lambda = 1550$ nm for $r = 1.5$ μm . (b) Schematic of WDM link from single waveguide, modulating multiple signals, ring filter demultiplexing array and dropping to multiple waveguides ending in detectors. (c) Radiation loss and maximum loaded Q solved at $\lambda = 1.55$ μm . The minimum useful radius is 1.7 μm . (d) Effective index 2D color contour plot. Black contour lines: solutions for resonator condition $n_{eff} = m\lambda / 2\pi r$. A maximum bandwidth of 50 nm is achieved with radii spanning from 1.802 μm to 1.903 μm .

We demonstrate that the silicon microring modulator has an FSR-limited WDM bandwidth of 50 nm due to its minimum radius of $r = 1.7$ μm . It was suggested by Xu et al. [4] that the minimum radius to obtain a microring with moderately high quality factor Q is $r \approx 1.5$ μm . However, this calculation did not include a silicon slab for electrical access which increases the radiation loss. We include a 30 nm Si slab in an FEM modesolver simulation, shown in Fig. 1(a). In Fig. 1(c) we calculate radiation loss $\alpha = 4\pi\text{Im}\{n_{eff}\} / \lambda$ at $\lambda = 1.55$ μm , and the corresponding maximum critically coupled $Q_{loaded} = \pi n_g / \lambda \alpha$. We find that radiation-limited $Q_{loaded} > 10,000$ is achievable for devices with radius $r > 1.7$ μm . In Fig. 1(d) we show a 2D color contour plot of the real part of $n_{eff}(\lambda, r)$ with black lines satisfying the mode condition $n_{eff} = m\lambda / 2\pi r$. The solid white line shows a range of resonances covering the C-band. We find the FSR (dotted white line) to be 50 nm (6.3 THz). This determines the maximum bandwidth available for WDM channels without the $m=1$ mode of the smallest resonator interfering with the m mode of the largest resonator (dashed white line).

WDM Channel Spacing

Next we consider how many channels can fit into the available 50 nm bandwidth. As wavelength channels are placed closer together, we examine the resulting loss and crosstalk for a modulator, an array of modulators, and an array of demultiplexing filters interacting with each other. We solve for the resonator spectra using the $n_{eff}(\lambda)$ data from Fig. 1(d). For modulators, the resonance shift from electrons and holes is incorporated by adding the silicon material free carrier dispersion (FCD) and absorption (FCA) [5] multiplied by the waveguide's silicon confinement factor.

We show that a single microring modulator must be shifted by more than one linewidth to obtain insertion loss $IL < 1$ dB. We start by choosing a microring with $r = 1.8725$ μm , and resonant wavelength at $\lambda_0 = 1550$ nm. We choose coupling and propagation loss such that the resonator has a linewidth $\Delta\lambda_{FWHM} = 0.15$ nm ($Q_0 = \lambda_0 / \Delta\lambda_{FWHM} \approx 10,000$) and 20 dB extinction ratio. We find that when free carriers are added shifting by one linewidth (0.15 nm) results in $IL = -1.1$ dB. Shifting by 2 or 3 linewidths results in $IL = -0.36$ dB and -0.18 dB, respectively, but will increase the modulator power consumption due to increased carrier concentration (see appended page). Next we examine the insertion loss induced by neighboring modulators in a WDM configuration where different

resonators are coupled to the same bus waveguide. In Fig. 2(a) we show insertion loss versus channel spacing. The different lines show results for different choices of modulator shifting. For a modulator shift of 2 linewidths, we find $IL = -0.84$ dB, -0.55 dB, and -0.42 dB for 0.6 nm, 0.8 nm, and 1.2 nm spacing respectively.

The interchannel crosstalk in a demultiplexing array of microrings for a WDM receiver is affected by the proximity of the channels. We find that a channel spacing of 0.8 nm (100 GHz) is required to achieve < -20 dB of crosstalk for $Q = 10,000$. An array of microrings with drop ports can be used to demux the wavelength channels and send each to a photodetector. In Fig. 2(b) we plot an example of individual drop port responses for microrings in an array with 0.6 nm channel spacing. Here we use $\alpha = 3$ dB/cm and select the waveguide coupling to obtain $Q_0 = 10,300$ (linewidth = 0.15 nm) to match the modulators. We find an insertion loss $IL_0 = -0.36$ dB on resonance, and the neighboring channel has $IL_1 = -18.5$ dB at 1550 nm. We define the crosstalk from Ch0 on neighboring Ch1 as $XT_{10} = IL_1 - IL_0$ dB. In Fig. 2(c) we plot crosstalk versus channel spacing. The nearest neighbor crosstalk XT_{10} is -18.1 dB at 0.6 nm spacing, -20.6 dB at 0.8 nm spacing, and -24.1 dB at 1.2 nm spacing. For example, requiring -20 dB crosstalk results in 50 nm / 0.8 nm = 62 wavelength channels. Crosstalk of -30 dB requires 2.4 nm spacing, resulting in only 20 allowed wavelength channels. The data in Fig. 2(c) can be applied to resonators with different Q (different linewidth) using the top axis in units of resonator linewidth. To improve the crosstalk performance, higher-order filters with multiple rings could be used to obtain steeper filter roll-off.

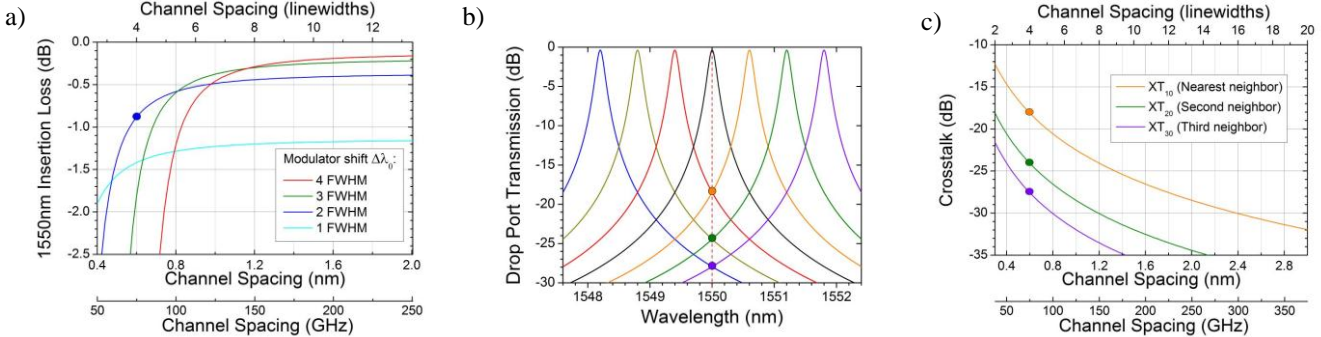


Fig. 2. Loss and crosstalk calculations for a modulator array (a), and demux array (b-c). All plots have $Q_0 = 10,300$ (linewidth = 0.15 nm). (a) Modulator array worst-case insertion loss at 1550 nm versus channel spacing. (b) Crosstalk at detector demultiplexer. Spectra for demux microring array with 0.6 nm channel spacing. (c) Crosstalk from the 1550 nm wavelength channel on the three nearest neighbors.

Channel Power Limit

We determine the maximum power that each channel can carry due to nonlinear losses. Sufficient optical power must reach a receiver to meet sensitivity requirements for error-free operation, but optical power cannot be made arbitrarily high because nonlinear effects will add increasing levels of loss and crosstalk. High optical intensities are possible in both bus waveguides (where many wavelength channels are multiplexed) and small high- Q cavities (where power builds considerably). The primary nonlinear loss mechanisms in silicon are two-photon absorption (TPA) and the resulting FCA from optically generated electrons and holes [5,6].

We find the maximum power per wavelength to be 1.5 mW due to unwanted resonance shift from FCD in a minimal-sized resonator with $Q = 10,000$. We solve for the nonlinear change in transmission for light on-resonance as the power is increased. At 1.5 mW input power, 7.3×10^{15} cm⁻³ carriers are generated which blueshift the resonance by 23 pm due to FCD. This significantly degrades the off state extinction ratio to -10 dB.

In a bus waveguide, nonlinear losses will depend on both the power in each channel and the number of channels. We take into account losses from both degenerate and non-degenerate TPA, as well as FCA from the optically generated carriers. With the modulator power limited to 1.5 mW/channel and a maximum number of 62 wavelengths (giving 93 mW total power), the excess nonlinear loss through 1 cm of propagation is 0.49 dB when all wavelengths are on. The power at each wavelength is low enough that we do not consider crosstalk from individual wavelength channels [7], but instead consider the worst-case aggregate nonlinear loss to be included in the power budget.

Conclusion

We discussed the limits of device performance for designing realistic optical systems that use silicon microring resonators as first-order filters for modulation and demux functions. For maximum utilization of the 50 nm WDM bandwidth balanced with reasonable loss and crosstalk values, the recommended parameters are 0.8 nm minimum wavelength spacing, 62 maximum wavelength channels, and 1.5 mW maximum optical power per wavelength at the modulator. Systems utilizing these devices can conceivably transmit Tbps data rates through a single optical waveguide.

- [1] A. Shacham, K. Bergman, and L. P. Carloni, "Photonic Networks-on-Chip for Future Generations of Chip Multiprocessors," *IEEE Trans. Comput.* **57**, 1246-1260 (2008).
- [2] P. Koka et al., "Silicon-photonic network architectures for scalable, power-efficient multi-chip systems," in *Proceedings of the 37th Annual International Symposium on Computer Architecture*, (ACM, Saint-Malo, France, 2010), pp. 117-128.
- [3] Q. Xu, B. Schmidt, S. Pradhan, and M. Lipson, "Micrometre-scale silicon electro-optic modulator," *Nature* **435**, 325-327 (2005).
- [4] Q. Xu, D. Fattal, and R. G. Beausoleil, "Silicon microring resonators with 1.5-μm radius," *Opt. Express* **16**, 4309-4315 (2008).
- [5] R. Soref and B. Bennett, "Electrooptical effects in silicon," *IEEE J. Quantum Electron.* **23**, 123-129 (1987).
- [6] T. K. Liang and H. K. Tsang, "Role of free carriers from two-photon absorption in Raman amplification in silicon-on-insulator waveguides," *Appl. Phys. Lett.* **84**, 2745-2747 (2004).
- [7] Y. Okawachi et al., "Optical Crosstalk in Silicon Nanowaveguides," OFC 2010, paper JWA21.

Appendix: Modulator Constraints

The parameters used to calculate WDM requirements are based on the use of a PIN diode or PN depletion-type modulator, typical for fast modulation with silicon microrings. Injection of electrons and holes into the resonator decreases the refractive index by Δn and blueshifts the resonant wavelength by $\Delta\lambda_0$ via the plasma dispersion effect. In Fig. A1(a) we plot the power transmission $|E_{\text{through}}/E_{\text{in}}|^2$ for a microring with $r = 1.8725 \mu\text{m}$ with resonant wavelength at $\lambda_0 = 1550 \text{ nm}$. The insertion loss due to resonance shift is highlighted.

In Fig. A1(b) we show this insertion loss as a function of resonance shift, along with corresponding free carrier concentration. We plot the insertion loss at 1550 nm wavelength from which we can determine the modulator power necessary for a given amount of loss. The insertion loss in dB is well fit by the function $IL = ax^b$ where x is resonance shift $\Delta\lambda_0$ in units of linewidths, $a = -1.0775$, and $b = -1.6061$. By using units of linewidths on the top axis, the IL data can be applied to resonators with different Q (with a small error due to free carrier absorption effects at different carrier concentrations).

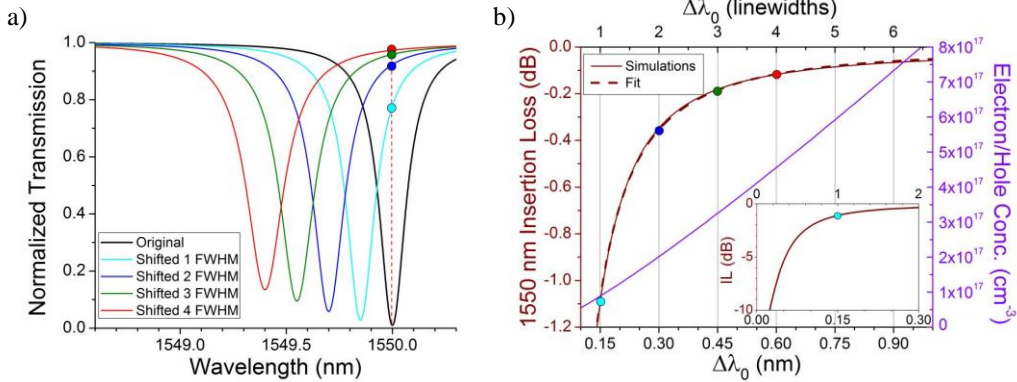


Fig. A1. Insertion loss from modulator resonance shift. (a) Microring modulator with $Q_0 = 10,300$ (linewidth = 0.15 nm) and with increasing electron and hole concentration to shift the resonant wavelength by 1 \times , 2 \times , 3 \times , and 4 \times the original linewidth $\Delta\lambda_{\text{FWHM}}$. (b) Insertion loss at 1550 nm and the associated electron and hole concentration as a function of resonance shift $\Delta\lambda_0$. Shifting by only 1 linewidth results in 1.1 dB insertion loss. Inset: Expansion of insertion loss data down to smaller wavelength shifts.

The total transmission through multiple resonators sharing a bus waveguide can then be computed by multiplying their transmission functions, where the loss will be given by the overlap of the tails of the Lorentzian functions. The grey line in Fig. A2 shows the spectrum for many cascaded modulators with 0.6 nm (75 GHz) channel spacing which are all turned off. The graph is centered on modulators with radii $r_1 = 1.8713 \mu\text{m}$ and $r_3 = 1.8738 \mu\text{m}$ for this channel spacing. The blue curve shows the worst-case insertion loss when Ch2 is on; this happens when modulators at shorter wavelengths are off and modulators at longer wavelengths are on, putting their resonances the closest to Ch2. (Here we shift by 2 linewidths to turn on a modulator.) At 1550 nm we find an insertion loss of -0.84 dB, which may be too large for some systems.

We note that the insertion loss in Fig. A2 will fluctuate in time between a “best-case” and “worst-case” value based on the state of the neighboring modulators. Here we have shown the worst-case insertion loss value, which is equivalent to the maximum power penalty at the receiver to achieve error-free operation. In general, the insertion loss can be overcome by increasing the optical power to meet the receiver sensitivity requirements; however we find ourselves limited by the optical power constraints inside silicon nanophotonic devices. We need to always remember that the trade-offs between channel spacing, insertion loss, and optical power can be optimized for any given system or network architecture.

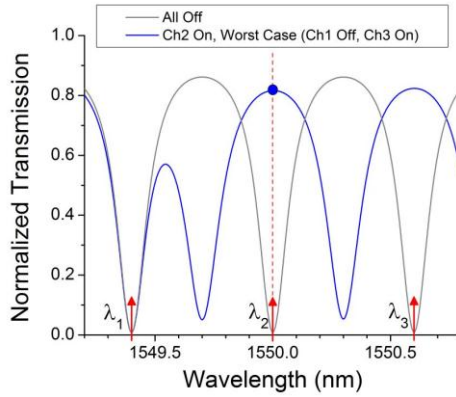


Fig. A2. Total modulator insertion loss including neighboring modulators. Spectra for modulator array with $Q_0 = 10,300$ (linewidth = 0.15 nm) and 0.6 nm channel spacing. We shift by 2 linewidths to turn on the modulators. Grey line: spectrum for all channels off. Blue line: Worst-case insertion loss for Ch2 (with Ch1 and lower modulators off, and Ch3 and higher modulators on).